Deposition of Highly Ordered CF_2-Rich Films Using Continuous Wave and Pulsed Hexafluoropropylene Oxide Plasmas

Carmen I. Butoi, Neil M. Mackie, Lara J. Gamble,† David G. Castner,† Jeffrey Barnd, Anne M. Miller, and Ellen R. Fisher*

Department of Chemistry, Colorado State University, Fort Collins, Colorado 80523-1872

Received March 20, 2000. Revised Manuscript Received May 15, 2000

The structure and composition of fluorocarbon materials deposited in pulsed and continuous wave (CW) hexafluoropropylene oxide (HFPO) plasmas were investigated. Results indicate substantial dependence on substrate position relative to the rf coil. When the substrate was placed 8 cm downstream from the rf coil (25 W CW), highly amorphous, cross-linked films were obtained. In contrast, materials deposited 28 cm downstream from the rf coil contained less cross-linked moieties and a higher degree of order. Angle-resolved X-ray photoelectron spectroscopy (XPS) C_{1s} analysis showed that the 28 cm materials contain up to ~80% CF_2 and CF_3 surface-enriched layers. Static secondary ion mass spectroscopy (SIMS) data revealed that these fluorocarbon materials are composed of long CF_2 chains. Near edge X-ray absorption fine structure (NEXAFS) analysis showed that the CF_2 chains were oriented perpendicular to the substrate surface for the films deposited at 28 cm downstream, while the films obtained 8 cm downstream do not exhibit any particular orientation. The compositions of materials deposited in pulsed HFPO systems have rf power and distance dependencies similar to those observed in the CW plasmas.

I. Introduction

Over the past 20 years, pulsed rf plasmas have been successfully employed in plasma polymerization of a variety of monomers.[1,2,3] With pulsed plasma polymerization, high retention of the monomer functional group in the resulting polymeric film can be achieved.[4] In addition, pulsed plasmas provide access to lower continuous wave (CW) equivalent powers because the rf power is on for only a portion of the cycle time. Use of pulsed sources reduces trapped radicals in the film, lowers deposition surface temperatures, decreases high-energy ion bombardment and UV flux to the surface, and provides greater control over the resulting film chemistry.[5] In contrast, films deposited from CW plasmas are often amorphous polymeric materials with little resemblance to the original monomer.[6,7] This is partially because CW plasmas can significantly fragment and scramble monomer functional groups through complex recombination and addition reactions.[8] However, materials generated at very low CW powers have been shown to retain some monomer functionalities.[9] Alternatively, we have previously reported the use of pulsed rf plasmas to produce a variety of hydrogenated and fluorinated organic films with a high degree of controllability over film composition.[4]

Alternatives to pulsed plasma film deposition are provided by plasma-enhanced chemical vapor deposition (PECVD) using downstream and remote CW plasmas, which also decrease energetic species bombardment of the deposited material. Again, this eliminates undesired effects usually associated with the use of CW plasmas and can produce films with unique properties.[10,11,12] Fluorocarbon materials deposited in this manner have been shown to possess low dielectric constants[13] and increased biocompatibility.[14,15] O'Kane and Rice reported pronounced composition differences between films generated at different distances from the rf glow

† Department of Bioengineering and Chemical Engineering, University of Washington, Box 1750, Seattle, WA 98195-1750.

(1) Yasuda, H.; Hsu, T. *J. Polym. Sci., Polym. Chem. Ed.* **1977**, *15*, 81−87.
(2) Rinsch, C. L.; Chen, X.; Panchalingam, V.; Eberhart, R. C.; Wang, J. H.; Timmons, R. B. *Langmuir* **1996**, *12*, 2995.
(3) Savage, C. R.; Timmons, R. B.; Lin, J. W. In *Structure−Property Relations in Polymers*; Advances in Chemistry Series 236; American Chemical Society: Washington, DC, 1993; p 745.
(4) Mackie, N. M.; Castner, D. G.; Fisher, E. R. *Langmuir* **1998**, *14*, 1227−1235. Mackie, N. M.; Fisher, E. R. *Polym. Prepr.* **1997**, *38*, 1059. Leich, M. A.; Mackie, N. M.; Williams, K. L.; Fisher, E. R. *Macromolecules* **1998**, *31*, 7618−7626. Lefohn, A. E.; Mackie, N. M.; Fisher, E. R. *Plasmas Polym.* **1998**, *4*, 197.
(5) Panchalingam, V.; Chen, X.; Savage, C. R.; Timmons, R. B.; Eberhart, R. C. *J. Appl. Polym. Sci., Polym. Symp.* **1994**, *54*, 123.
(6) Yasuda, H. *Plasma Polymerization*; Academic Press: Orlando, FL, 1985.
(7) Mackie, N. M.; Dalleska, N. F.; Castner, D. G.; Fisher, E. R. *Chem. Mater.* **1997**, *9*, 349.
(8) *Plasma Deposition, Treatment and Etching of Polymers*; d'Agostino, R., Ed.; Academic Press: Boston, 1990.
(9) Alexander, M. R.; Duc, T. M. *J. Mater. Chem.* **1998**, *8*, 937.
(10) Castner, D. G. In *Plasma Processing of Polymers*; d'Agostino, R., Favia, P., Fracassi, F., Eds.; Kluwer Academic Publishers: Dordrecht, The Netherlands, 1997; pp 221−230.
(11) O'Kane, D. F.; Rice, D. W. *J. Macromol. Sci. Chem. A* **1976**, *10*, 567.
(12) Yasuda, H. *J. Polym. Sci. Macromol. Rev.* **1981**, *16*, 199.
(13) Singer, P. *Semicond. Int.* **1996**, *May*, 88−96.
(14) Bohnert, J. L.; Fowler, B. C.; Horbett, T. A.; Hoffman, A. S. *J. Biomater. Sci., Polym. Ed.* **1990**, *1*, 279.
(15) Kiaei, D.; Hoffman, A. S.; Horbett, T. A. *J. Biomater. Sci., Polym. Ed.* **1992**, *4*, 35.

10.1021/cm0002416 CCC: $19.00 © 2000 American Chemical Society
Published on Web 06/16/2000

of a tetrafluoroethylene (TFE) plasma.[10] Fluoropolymers deposited at the longest distances contained the highest percentage of CF_2 and <5% CF_3. Castner and co-workers found that depositions performed downstream from the discharge glow in a TFE plasma produced highly ordered materials with high CF_2 content.[16]

Along with TFE plasmas, other fluorocarbon systems have been utilized for the deposition of polymeric films with low dielectric constants as well as for producing biocompatible materials.[17,18,19] One monomer that has been used extensively in pulsed plasma polymerization work is hexafluoropropylene oxide (HFPO). Timmons and co-workers deposited films in HFPO plasmas under pulsed conditions but observed no film formation at 300 W under CW conditions.[20] Gleason and co-workers also found that the use of pulsed HFPO plasmas (0.5% duty cycle, 280 W) results in high CF_2 content fluoropolymers. In contrast to Timmons' results, Gleason's group did observe film formation under CW conditions (120 W), but these films were highly cross-linked, unlike those obtained in the pulsed plasma system.[21] Neither Timmons' nor Gleason's studies probed film orientation with respect to the substrate surface.

An earlier communication from our laboratory presented limited results for films deposited in CW HFPO plasmas.[22] The present work aims to provide a more comprehensive perspective into the nature of films deposited in HFPO plasmas under CW as well as pulsed conditions. To identify the best conditions for the deposition of highly ordered, CF_2-rich materials, plasma parameters were varied along with distance from the discharge visible glow for both CW and pulsed systems. Film composition was investigated with Fourier transform infrared (FTIR) spectroscopy, angle-resolved X-ray photoelectron spectroscopy (XPS), and static secondary ion mass spectrometry (SIMS), while near-edge X-ray absorption fine structure (NEXAFS) analysis was used to determine structural attributes. We have also determined film deposition rates under different plasma conditions and tested the mechanical stress properties of fluoropolymers deposited on Cu wires.

II. Experimental Methods

All films were deposited in our home-built inductively coupled rf plasma reactor, described in detail previously.[7,23] For the present work, the reactor was modified by extending one glass tube section to allow for downstream depositions (Figure 1). Input power for CW depositions was varied from 5 to 120 W, and the applied peak power was kept constant at 300 W for pulsed experiments. In the latter case, the equivalent CW power can be determined by calculating the time averaged power applied over the entire pulse cycle. A 10/190 ms pulse sequence, where the plasma is on for 10 ms and off for 190 ms, corresponds to an equivalent CW power of 15 W and a duty cycle of 5%. The pulse duty cycle (defined as the ratio of pulse on time to the total cycle time) was varied using the internal pulse generator of an RF Power Products power supply. For each deposition, a freshly pressed FTIR grade KBr (Aldrich) pellet and a silicon wafer (p-type, 110) with 40−60 Å of native oxide were used as substrates. These were placed on glass microscope slides oriented parallel to the gas flow within the coil region (position A, Figure 1) as well as at 8 and 28 cm downstream (positions B and C, respectively, in Figure 1). CW and pulsed deposition times ranged from 30 min to 2 h. For pulsed experiments, deposition time was defined by the total time the sample was exposed to both pulse on and off cycles.

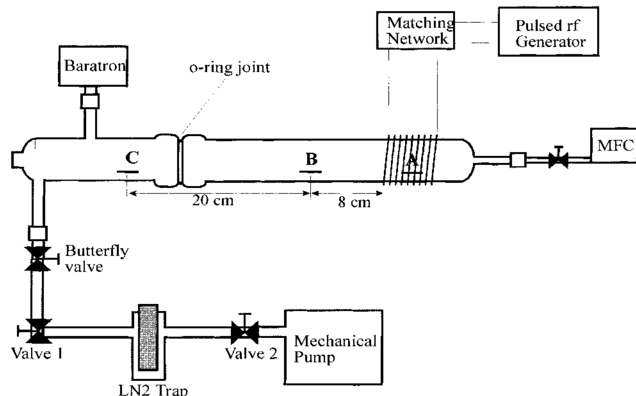

Figure 1. Schematic diagram of the inductively coupled rf plasma reactor used for all depositions. The HFPO flow is controlled by a mass-flow controller (MFC). Substrates placed at position A are within the visible glow. Positions B and C correspond to substrate positions 8 and 28 cm downstream from the rf coil, respectively.

Transmission FTIR spectral analysis on films deposited on KBr pellets and Si wafers was performed ex situ using a Nicolet Magna 760 FTIR spectrometer (resolution of 8 cm^{-1} and averaging 128 scans). Spectra shown are corrected for residual carbon dioxide not purged from the FTIR spectrometer (absorbances at ~2340 and 2360 cm^{-1}).

XPS analyses were performed on a Surface Science Instruments S-probe spectrometer located at the University of Washington NESAC-BIO center. This system has a monochromatic Al Kα X-ray source ($h\nu$ = 1486.6 eV), a hemispherical analyzer, and a resistive strip multichannel detector. A low-energy (~5 eV) electron gun was used for charge neutralization on the nonconducting samples. The binding energy (BE) scales for the samples were referenced by setting the CF_2 peak maxima in the C_{1s} spectra to 292.0 eV. High-resolution C_{1s} spectra were acquired at an analyzer pass energy of 50 eV and an X-ray spot size of 1000 μm and were fit using Gaussian functions with fwhm of 1.3−1.5 eV. XPS elemental compositions were obtained using a pass energy of 150 eV. Photoelectron takeoff angles of 0, 55, and 80° were used; the takeoff angle is defined as the angle between the axis of the analyzer lens and the surface normal.

NEXAFS analysis was performed at the National Synchrotron Light Source at Brookhaven National Laboratory on beamline U7A. The 600 lines/mm grating monochromator was calibrated using the graphite $C_{1s} \rightarrow \pi^*$ transition (285.35 eV) and had an energy resolution of ~0.15 eV (fwhm) at the carbon K edge. Photoelectrons and Auger electrons were collected with a negatively biased channeltron to obtain partial electron yield (PEY) spectra. These spectra were normalized by using the PEY from a 90% transmission grid which was gold coated in situ and positioned in the incoming X-ray beam. The incidence angle is defined as the angle between the incident X-ray beam and the sample surface. Data were obtained at different incidence angles by rotating the sample with respect to the X-ray beam.

All time-of-flight SIMS (ToF-SIMS) spectra were acquired on a Physical Electronics PHI 7200 ToF-SIMS spectrometer. The instrument is equipped with a Cs^+ ion source operated at

(16) Castner, D. G.; Lewis, K. B.; Fischer, D. A.; Ratner, B. D.; Gland, J. L. *Langmuir* **1993**, *9*, 537−542.
(17) Endo, K.; Tatsumi, T. *Appl. Phys. Lett.* **1996**, *68*, 2864.
(18) Lee, W. W.; Ho, P. S. *MRS Bull.* **1997**, *22*, 19.
(19) Hoffman, A. S. *J. Appl. Polym. Sci.; Appl. Polym. Symp.* **1988**, *42*, 251.
(20) Savage, C. R.; Timmons, R. B. *Chem. Mater.* **1991**, *3*, 575.
(21) Limb, S. J.; Edell, D. J.; Gleason, E. F.; Gleason, K. K. *J. Appl. Polym. Sci.* **1998**, *67*, 1489.
(22) Butoi, C. I.; Mackie, N. M.; Barnd, J. E.; Fisher, E. R.; Gamble, L. J.; Castner, D. G. *Chem. Mater.* **1999**, *11*, 862.
(23) Bogart, K. H. A.; Dalleska, N. F.; Bogart, G.; Fisher, E. R. *J. Vac. Sci. Technol. A* **1995**, *13*, 476.

8 keV, a reflectron mass analyzer, and chevron-type multichannel plate detectors. For acquisition of spectra, a bunched primary Cs^+ beam (50 μm diameter, approximately 1 ns pulse width) is used, and the bin width of the time-to-digital converter (TDC) is set at 1.25 ns, resulting in mass resolutions ($m/\Delta m$) of >8000 at m/z = 27 for electrically conducting samples. The beam is rastered over a square area that is 100 μm on a side. Data acquisition times were adjusted to ensure that the spectra were taken in static mode, that is, that the total ion dose was $<2 \times 10^{12}$ ions/cm^2 during the acquisition.

Static contact angles for water were measured using the sessile drop method with a contact angle goniometer (Ramé Hart Model 100). Measurements were taken on both sides of water drops at ambient temperature, 30−40 s after 1 μL drops were applied to the surface and the needle tip was removed from each drop. For each sample, four drops were placed at different locations on the surface of the film. Each reported contact angle is an average of these measurements for three samples.

To investigate the morphology of the fluorocarbon materials deposited in HFPO plasmas, scanning electron microscope (SEM) images were obtained using a Philips 505 apparatus. The accelerating voltage was 26.0 kV, and the spot size was 20 nm. For more detailed morphological information, an atomic force microscope was utilized in tapping mode. The Digital Instruments Nanoscope III apparatus was used to measure root-mean-square (rms) surface roughness values on 5×5 μm^2 sample areas. Deposition rates were calculated using atomic force microscopy (AFM), ellipsometry, and profilometry analysis. For films with thickness > 500 Å, deposition rates were calculated on the basis of step height measurements with a Tencor Alpha Step 100 profilometer. Variable-angle spectroscopic ellipsometry (J. A. Woollam Company Inc., model HS 190) and AFM analysis were used to determine deposition rates for films thinner than 500 Å.

III. Results

A. FTIR Spectroscopy. Figure 2 shows FTIR spectra of films deposited at 8 cm (position B) and 28 cm (position C) downstream from the rf coil, using rf powers of 15, 30, and 60 W in a CW HFPO plasma. For materials deposited at position B at low rf powers (15 and 30 W), the spectra contain absorbance bands associated with amorphous plasma-polymerized fluorocarbon materials (Figure 2a). The most prominent feature in both spectra is the absorbance band at 1100−1400 cm^{-1}, attributable to all CF_x (x = 1−3) stretching modes.[24] The weaker absorbance band at 1700−1850 cm^{-1} corresponds to either $C{=}CF_2$ or $CF{=}CF_2$ moieties in the film.[23] In contrast, the film obtained from a 60 W CW plasma shows a feature corresponding to SiO stretching at ~1100 cm^{-1}, but very little CF_2 signal. The SiO band results from etching of the glass reactor walls followed by redeposition of the etched material on the KBr substrate.[7] This constitutes strong evidence that etching is the predominant plasma process at high rf powers.

Figure 2b shows FTIR spectra of films deposited at position C with applied rf powers of 15, 30, and 60 W. The spectra of materials obtained in 15 and 30 W CW plasmas are different from those shown in Figure 2a. Two distinct absorption bands at 1217 and 1165 cm^{-1}, corresponding to the CF_2 asymmetric and symmetric modes, respectively, are observed.[25] In addition, the

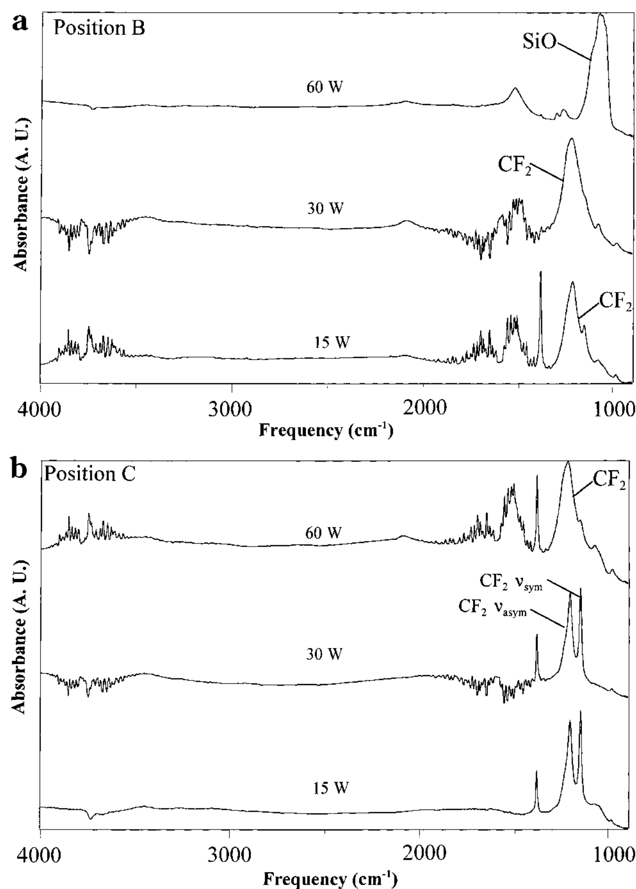

Figure 2. FTIR spectra of films deposited at (a) position B and (b) position C in a CW HFPO plasma at three different rf powers: 15, 30, and 60 W. The monomer gas pressure was 233 mTorr.

intensity of the $CF_x{=}CF_2$ (x = 0, 1) stretch at ~1700−1800 cm^{-1} is considerably lower in these films compared to what was observed in the films deposited at position B (Figure 2a). Along with the separation of CF_2 asymmetric and symmetric stretch bands, this indicates a lower degree of cross-linking than that of the fluorocarbon materials deposited at position B. In contrast, the FTIR spectrum of the 60 W film contains a broad absorption band at ~1200 cm^{-1}, consistent with a relatively amorphous fluorocarbon film.

The monomer pressure also affects the composition of materials deposited in our CW plasmas (Figure 3). Figure 3a displays the IR spectra for materials obtained at position B for a 30 W CW plasma and different HFPO pressures: 233, 490, and 900 mTorr. The presence of a broad band at ~1200 cm^{-1} indicates that the fluorocarbon film deposited at 233 mTorr is highly amorphous. For films generated at higher pressures, the symmetric and asymmetric CF_2 vibrational bands separate, consistent with the behavior of less amorphous materials. FTIR spectra of films deposited at position C, however, contain clearly separated CF_2 symmetric and asymmetric stretching bands at all monomer pressures (Figure 3b).

Figure 4 shows FTIR spectra of films deposited at positions A, B, and C using pulsed HFPO plasmas with different duty cycles. The spectrum of a film obtained at position A, at the highest duty cycle, 33% (10/23 ms), shows no absorbance band corresponding to the CF_x

(24) Seth, J.; Babu, S. V. *Thin Solid Films* **1993**, *230*, 90.
(25) d'Agostino, R.; Cramarossa, F.; Fracassi, F.; Illuzzi, F. In *Plasma Deposition, Treatment and Etching of Polymers*; d'Agostino, R., Ed.; Academic Press: San Diego, CA, 1990; pp 95−162.

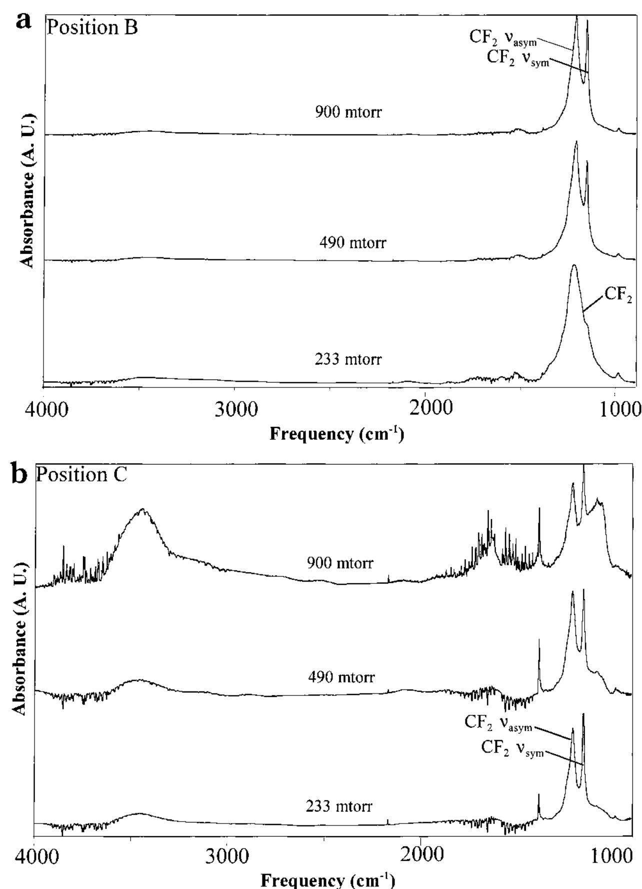

Figure 3. FTIR spectra for films deposited in a 30 W CW plasma at (a) position B and (b) position C using three different monomer pressures: 233, 490, and 900 mTorr.

stretching modes but does contain an SiO absorbance band (Figure 4a). This indicates that although a fluorocarbon film is not generated, material etched from the reactor walls is deposited on the substrate. The film produced at a lower duty cycle of 16% (10/52 ms) contains a broad band in the 1200−1300 cm^{-1} region as well as the SiO feature mentioned above. Thus, this material comprises both CF_x groups formed from the parent gas along with SiO moieties etched off the glass walls. The IR spectrum of the film deposited using a 5% duty cycle (10/190 ms) pulsed HFPO plasma, however, displays two distinct absorption peaks at 1217 and 1165 cm^{-1}, corresponding to CF_2 stretching modes. No other features are observed in the spectrum. Figure 4b indicates that, further downstream at position B, both the 5% and 16% duty cycle plasmas deposit fluorocarbon materials for which the CF_2 symmetric and asymmetric stretching bands are clearly separated. The IR spectrum of the film generated at the 33% duty cycle (10/23 ms) still exhibits the SiO peak caused by reactor wall etching along with a new broad shoulder in the 1200−1300 cm^{-1} region. This corresponds to the CF_2 vibrational signal and indicates that an amorphous material is obtained under these conditions. In contrast, at position C (Figure 4c), all three pulse sequences give rise to films whose IR spectra contain distinct CF_2 stretching bands and small degrees of unsaturation. Note that the IR spectra shown in Figure 4c are nearly identical to those of films deposited at position C in 15 and 30 W CW plasmas (Figure 2b).

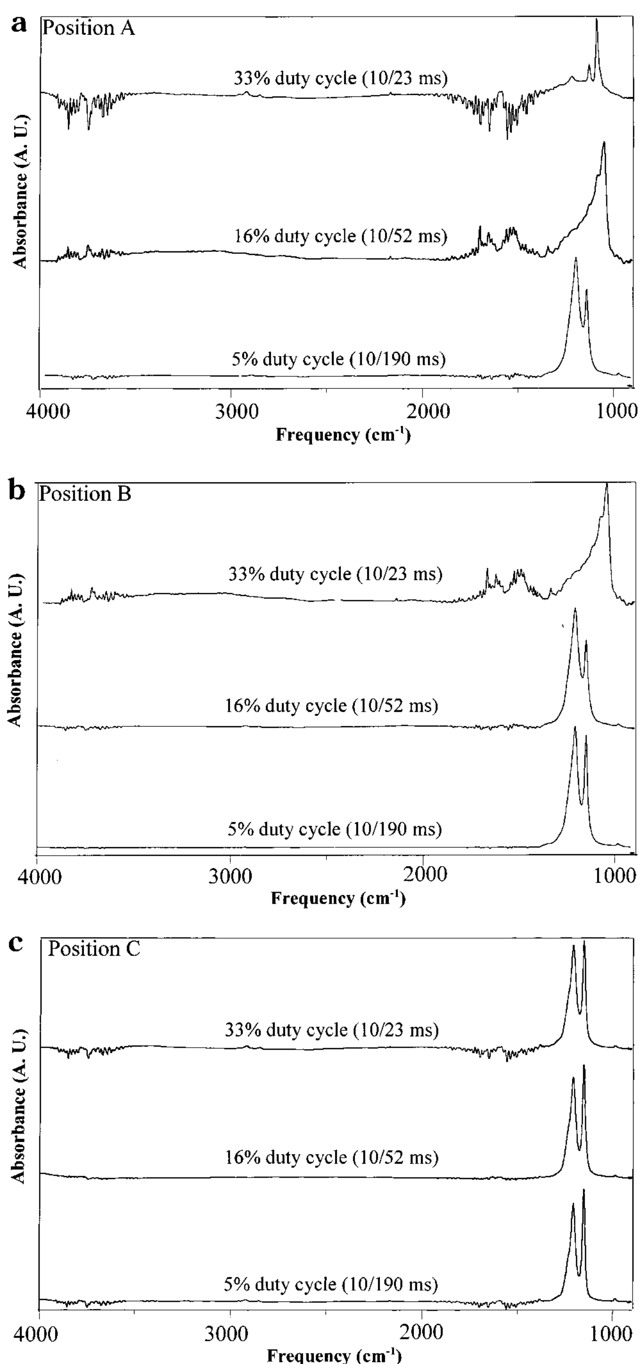

Figure 4. FTIR spectra of materials deposited at (a) position A, (b) position B, and (c) position C in pulsed plasmas with pulse sequences of 10/190 ms (5% duty cycle), 10/52 ms (16% duty cycle), and 10/23 ms (33% duty cycle). The monomer gas pressure was 233 mTorr.

B. XPS Analysis. Figure 5 shows the XPS spectra obtained at a 55° photoelectron takeoff angle for fluorocarbon films deposited at positions B and C in a 25 W CW plasma. Peaks corresponding to C−CF_x (287 eV), CF (290 eV), CF_2 (292 eV), and CF_3 (294 eV) moieties are present in the spectrum of the film generated at position B, with a content distribution of 39% (C−CF_x + CF), 36% (CF_2), and 25% (CF_3). In contrast, the sample deposited under the same plasma conditions but further downstream, at position C, contains significantly more CF_2 (80%) and less CF_3 (12%).

To investigate film composition as a function of sampling depth, materials generated at position C, in

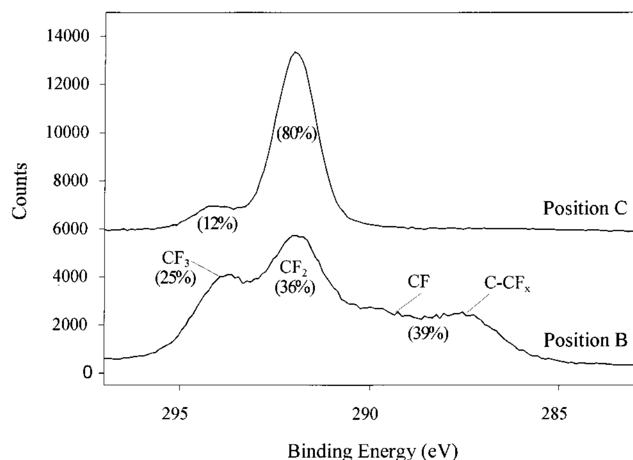

Figure 5. XPS C_{1s} spectra for films deposited at positions B and C in a 25 W CW plasma using a photoelectron takeoff angle of 55°. The percent content for CF_2, CF_3, and $C-CF_x$ groups is shown.

Table 1. Composition of Fluorocarbon Films Deposited on CW and Pulsed HFPO Plasmas[a]

	CF_2 (%)	CF_3 (%)	other (%)
25 W CW			
0°	76	12	12
80°	69	20	11
16% duty cycle			
0°	77	11	12
80°	72	14	16

[a] All films were deposited at position C. The composition was determined by angle-resolved XPS C_{1s} analysis.

both a 25 W CW and a 16% duty cycle (10/52 ms) pulsed plasma, were studied using two photoelectron takeoff angles, 0° and 80° (Table 1). The use of a 0° photoelectron takeoff angle provides information about the material composition ~90 Å deep, whereas, at an 80° angle, only the outermost surface layers of the film are probed. The C_{1s} analysis from these measurements is listed in Table 1. For the CW film, the 0° XPS data showed the approximate percentage of each species detected in the spectrum is 76% CF_2 and 12% CF_3. C=C and CF groups constitute the remaining 12%. As the photoelectron takeoff angle is increased to 80°, these percentages change significantly. The uppermost surface layers contained 69% CF_2 and 20% CF_3. Angle-resolved XPS analysis was also performed for materials generated in a 16% duty cycle pulsed plasma (Table 1). Here, the XPS data obtained at 0° indicate that the film contains ~77% CF_2 and ~11% CF_3. At 80°, XPS analysis revealed slightly lower CF_2 (74%) but higher CF_3 content (14%) for the outermost layers of the film.

We also investigated the composition of our films formed in the pulsed systems as a function of duty cycle and distance from the rf coil (Table 2). Two significant trends are apparent from the XPS analysis of these materials. First, for each reactor position, A, B, or C, the use of a higher duty cycle (shorter plasma off time) results in fluorocarbon materials with higher $C-CF_x$ content but lower CF_2 content. The amount of CF_3 present in the films also increases with increasing duty cycle (decreasing off times). Second, the closer the substrate is placed to the rf glow, typically the higher the degree of unsaturation and CF_3 content in the film, and the lower the CF_2 content. The 50% duty cycle

Table 2. Composition of Fluorocarbon Materials Deposited in Pulsed HFPO Plasmas As a Function of Distance from the rf Coil[a]

duty cycle (%)	position	CF_3 (%)	CF_2 (%)	CF (%)	CC (%)
5	A	13.0 ± 0.8	76.6 ± 1.1	6.8 ± 0.4	3.6 ± 0.6
	B	14.8 ± 0.5	73.6 ± 0.6	6.1 ± 1.1	5.4 ± 1.0
	C	13.8 ± 1.2	86.2 ± 1.2	0.0	0.0
16	A	18.9 ± 1.4	35.8 ± 2.8	19.7 ± 0.5	25.7 ± 2.9
	B	18.4 ± 0.4	56.6 ± 0.5	13.4 ± 1.3	11.6 ± 1.1
	C	11.5 ± 0.3	75.8 ± 0.4	5.2 ± 1.0	7.5 ± 1.3
50	A	9.1 ± 0.4	13.6 ± 1.0	12.5 ± 2.4	64.8 ± 3.7
	B	21.4 ± 1.4	31.7 ± 1.6	19.4 ± 0.5	27.4 ± 0.6
	C	15.2 ± 1.0	51.3 ± 0.7	13.9 ± 0.3	19.5 ± 1.2

[a] Determined from C_{1s} XPS analysis performed at a 55° takeoff angle.

Table 3. Elemental Composition for Films Deposited in CW and Pulsed HFPO Plasmas at Positions A, B, and C As Determined by XPS Analysis[a]

	C(1s)	F(1s)	O(1s)	Si(2s)	F/C
		25 W CW			
position a	28.6 ± 0.7	29.3 ± 0.4	15.2 ± 0.2	26.9 ± 0.7	1.0
position b	36.5 ± 0.1	62.3 ± 0.2	1.2 ± 0.2	0.0	1.7
position c	32.3 ± 0.9	63.4 ± 0.6	1.9 ± 0.4	2.3 ± 0.2	2.0
		5% Duty Cycle			
position a	33.3 ± 0.2	66.7 ± 0.2	0.0	0.0	2.0
position b	33.6 ± 0.5	66.4 ± 0.0	0.0	0.0	2.0
position c	33.0 ± 0.6	66.7 ± 1.1	0.3 ± 0.5	0.0	2.0
		16% Duty Cycle			
position a	39.8 ± 0.7	58.0 ± 1.3	1.8 ± 0.7	0.3 ± 0.5	1.5
position b	34.9 ± 0.5	64.8 ± 0.1	0.3 ± 0.4	0.0	1.9
position c	33.3 ± 0.2	66.4 ± 0.7	0.3 ± 0.5	0.0	2.0
		50% Duty Cycle			
position a	40.1 ± 1.8	35.8 ± 1.5	9.1 ± 0.7	9.1 ± 0.1	0.9
position b	36.0 ± 0.5	62.6 ± 0.6	1.4 ± 0.2	0.0	1.7
position c	35.9 ± 0.3	62.3 ± 0.3	1.8 ± 0.0	0.0	1.7

[a] Determined from XPS analysis performed at a 55° takeoff angle.

sample at position A does not follow some of these trends due to the presence of higher levels of glass and hydrocarbon contamination detected on this sample.

Table 3 shows the elemental composition for films generated in CW and pulsed HFPO plasmas as a function of distance from the rf coil. For materials obtained at position A in CW and high duty cycle pulsed systems, the highest amounts of Si and O are detected, indicating redeposition of SiO_2 etched from the walls of the glass reactor. This is consistent with what we observe in the FTIR spectra of these films. The higher Si content detected for the material generated at position C compared to the one at position B is most likely from the underlying Si substrate. For pulsed conditions, the Si and O content decreases with decreasing duty cycle. The most dramatic change in the F/C ratio with position occurs in the CW films. As the distance from the rf glow increases, the F/C ratio increases by a factor of 2. For the highest duty cycle (50%), a similar increase in F/C ratio is observed (Table 3). Although the same trend is observed in the 16% duty cycle data, the difference is much less pronounced. Interestingly, in the lowest duty cycle (5%) data, F/C = 2.0 at all substrate positions.

C. SIMS and NEXAFS Analysis. SIMS and NEXAFS analyses were employed to further characterize the composition and structure of materials generated in CW and pulsed HFPO plasmas. Figure 6 shows the SIMS

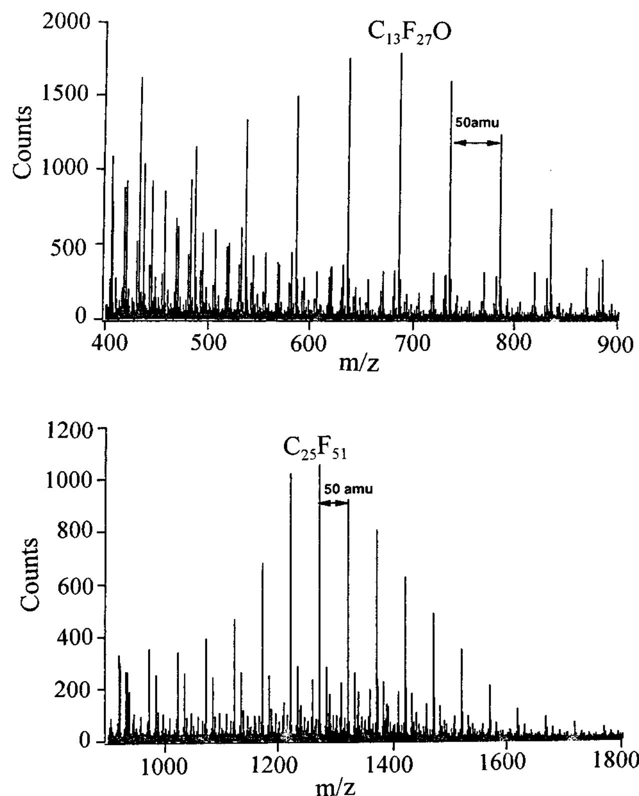

Figure 6. SIMS negative ion spectrum for the fluoropolymer deposited at position C in a 25 W CW system. As an example of an oxygen-containing ion, $C_{13}F_{27}O$ is annotated. Note that 50 amu corresponds to one CF_2 unit.

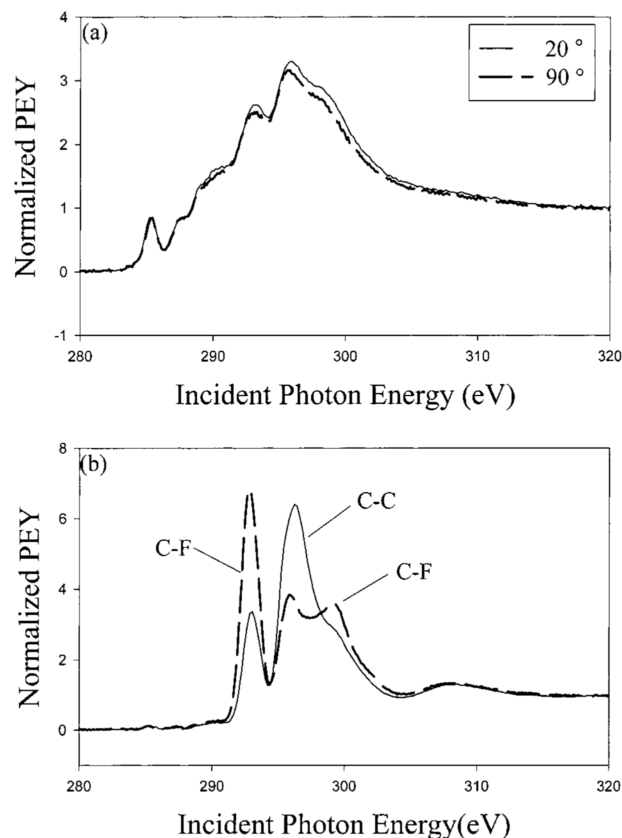

Figure 7. NEXAFS spectra for films deposited at (a) position B and (b) position C in a 25 W CW plasma. Results for two X-ray angles of incidence are shown: 20° (solid line) and 90° (dotted line).

spectrum for a film deposited at position C in a 25 W CW plasma. The presence of OC_nF_{2n+1} molecular ions ($C_{13}F_{27}O$ is annotated in Figure 6) is consistent with some oxygen incorporation in the films deposited at position C. This agrees well with the XPS data given in Table 3. Oxygen incorporation was not observed for downstream depositions when a nonoxygenated fluorocarbon monomer (i.e. TFE) was employed.[15] In the 1000−1800 amu region, the series of peaks separated by 50 amu (i.e. CF_2 groups) correspond to C_nF_{2n+1} molecular ions. The persistence of these mass peaks out to very high masses indicates the presence of long CF_2 chains in our films. For comparison, the films produced by Castner and co-workers showed a similar trend, with molecular ions corresponding to additions of CF_2 units up to at least 250 amu.[15] One important note is that since the secondary ion yield for OC_nF_{2n+1} can be significantly different than that for C_nF_{2n+1}, the relative intensities of the fragment signals are not indicative of the relative concentrations of the two species.

To determine the orientation of these chains with respect to the substrate surface, NEXAFS analysis was employed. Figure 7a shows the NEXAFS spectra of a film deposited in a 25 W CW plasma at position B. Data obtained at 20° (grazing) and 90° (normal) incidence angles are presented. Absorption features assigned to transitions of C−F (292 and 298 eV) and C−C (295 eV) core electrons to σ^* orbitals are observed. There is no difference in the intensity of these features between the 20° and 90° spectra, indicating no particular orientation of the C−F and C−C bonds. Similar behavior is observed for films deposited at position A. This is not true, however, for films deposited at position C (Figure 7b). Here, the intensity of the C−F absorption bands decreases as the angle between the substrate and X-ray beam changes from 90° to 20°. This type of decrease is consistent with C−F bonds oriented parallel to the substrate surface. In contrast, the C−C peak intensity is lowest when the X-ray is perpendicular to the film surface, showing that the helical axis of the C−C backbone is perpendicular to the C−F bonds in the film. These NEXAFS results along with the SIMS data indicate that the fluoropolymers deposited at position C comprise long CF_2 chains which are oriented normal to the substrate surface. Clearly, long CF_2 chains are also deposited at the other positions, but the perpendicular orientation of the chains is observed only in the films deposited at position C.

A similar CF_2 chain orientation dependence on distance from the rf glow occurs with films deposited in pulsed HFPO plasmas. Films obtained at position C contain chains which are perpendicular to the substrate surface while those generated at positions A and B show very little or no particular orientation. The effect of duty cycle on film structure was also studied. The difference in 20° and 90° NEXAFS peak intensity is largest in Figure 8a, which corresponds to a film produced in a 5% duty cycle plasma system. No particular orientation of the 50% duty cycle film was observed at position B, but a small degree of orientation was detected for the 16% and 5% duty cycle films at position B. These data demonstrate that materials deposited at position C have the highest degree of order for the lowest duty cycle,

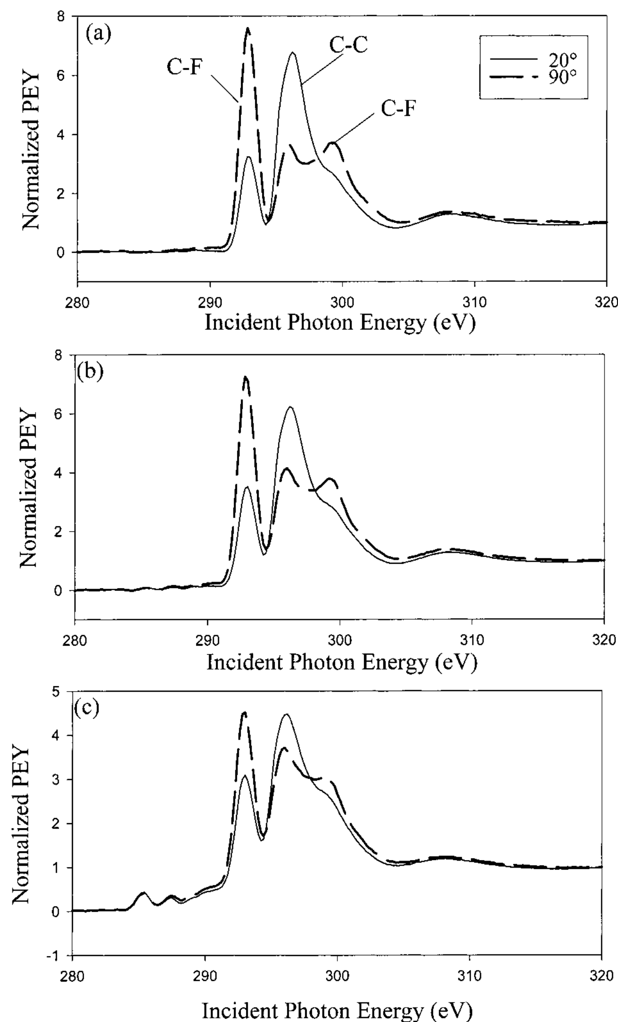

Figure 8. NEXAFS spectra for films deposited at position C in pulsed plasmas with duty cycles of (a) 5%, (b) 16%, and (c) 50%. The angles of incidence were 20° (solid line) and 90° (dotted line).

5% (10/190 ms). As the duty cycle increases to 16% (10/52 ms) and 50% (10/23 ms) (Figure 8b and c, respectively), this difference decreases. Thus, a lower degree of CF_2 chain ordering is observed as the plasma off time decreases (duty cycle increases).

D. Contact Angle. To determine the wettability of film surfaces, static contact angles were measured for materials deposited at positions B and C in CW plasmas with different applied rf powers (Figure 9). At applied powers ≥60 W, the contact angles of films generated at position C are nearly identical to those deposited at position B. All films deposited at rf powers <60 W are hydrophobic (contact angles of 105–117°), but those deposited far downstream, at position C, have higher contact angles than the films deposited at position B. These data support the XPS analysis findings, because the higher hydrophobicity of films generated at position C is likely caused by increased CF_3 incorporation at the film surface. Indeed, CF_3 moieties have been shown to contribute to the hydrophobicity of fluorinated films.[23]

Contact angles were also measured for fluorocarbon materials deposited in pulsed plasmas at duty cycles ranging from 2% to 50% (Figure 10). At low duty cycles, when the plasma is off for long times, no difference in

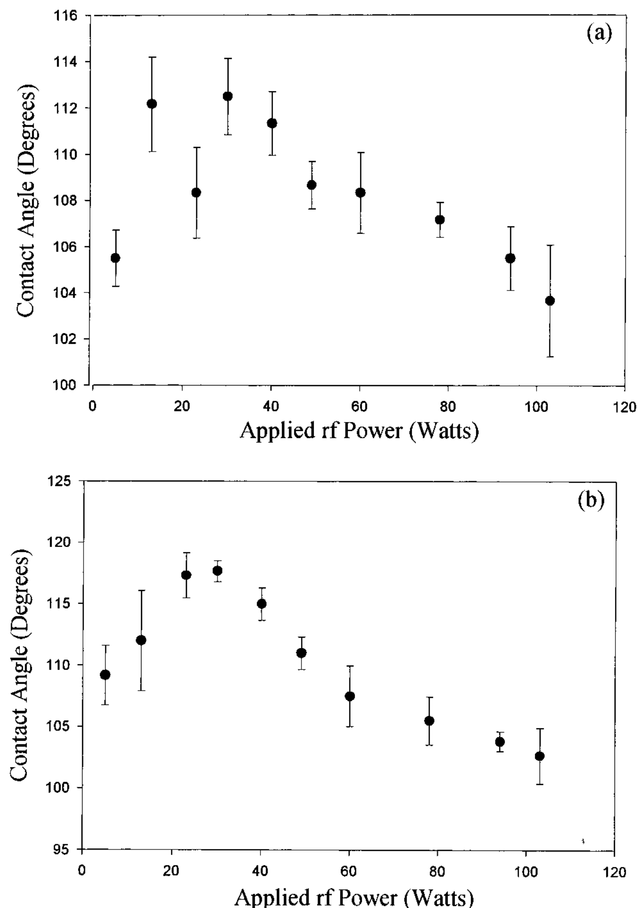

Figure 9. Dependence of the static contact angle on applied rf power for films deposited in CW plasmas at (a) position B and (b) position C. The monomer gas pressure was 233 mTorr.

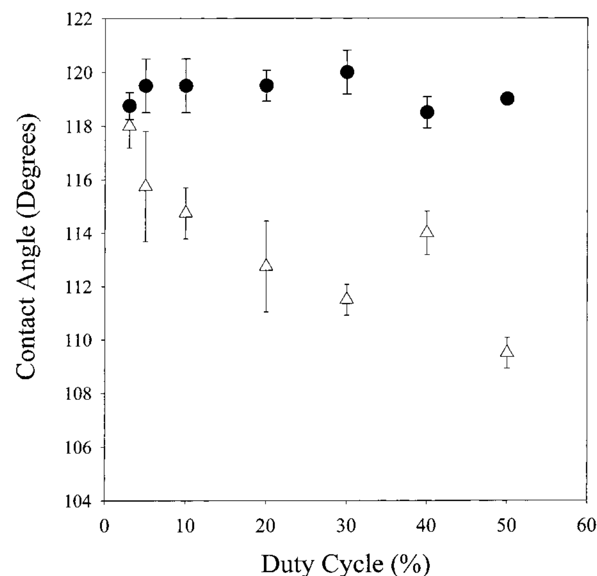

Figure 10. Dependence of the static contact angle on duty cycle for films deposited in pulsed plasmas at position B (open triangles) and position C (closed circles). The monomer gas pressure was 233 mTorr.

contact angle is observed for films generated at positions B and C. However, position C films are more hydrophobic than position B materials when duty cycles > 5% are employed. As with the CW films, this is likely due to more surface CF_3 incorporation in films deposited at position C relative to position B.

Table 4. Film Deposition Rates (Å/min) in CW and Pulsed HFPO Plasmas

	position B	position C
25 W CW	7 ± 1	1.6 ± 0.3
16% duty cycle	50 ± 5	17 ± 3
50% duty cycle	183 ± 8	52 ± 3

E. Deposition Rates. Table 4 lists the deposition rates measured for materials generated in a 25 W CW plasma at positions B and C. A relatively high deposition rate of 30 Å/min is observed at position B compared to the 1.6 Å/min observed at position C. The low thickness for films generated at position C explains the higher Si content detected by XPS compared to that for the materials generated at position B. For comparison, we also measured deposition rates in pulsed plasma systems. As shown in Table 4, these deposition rates are higher for materials generated at both positions B and C, relative to what was observed for CW systems. Indeed, at position C, there is an order of magnitude increase in the deposition rate for the 16% duty cycle pulsed system compared to the 25 W CW system. Also important to note, deposition rates are higher closer to the glow under all plasma conditions (CW and pulsed).

F. SEM and AFM Imaging. We have investigated the mechanical flexibility of the fluorocarbon films deposited in HFPO plasmas by coating a 200 μm copper wire placed at position C under both CW and pulsed conditions. In Figure 11a the SEM image of a wire coated in a 5% duty cycle pulsed plasma shows a very smooth film. Figure 11b displays the same wire after it has been bent in a loop ~0.5 cm in diameter. No significant cracking of the fluorocarbon coat is observed, suggesting that the material has a high degree of flexibility. Figure 11c shows a similar wire that was coated in a 25 W CW plasma and bent into a loop. Just as for the film produced under pulsed conditions, bending does not result in any noticeable film deterioration.

AFM imaging was used to determine the surface rms roughness for materials deposited in CW and pulsed HFPO plasmas at positions A, B, and C. Values ranged from 2 to 20 nm, comparable to the 0.88−31.7 nm range reported by Gleason and co-workers.[26] For Gleason's materials, the lowest rms roughness of 0.88 nm was measured for materials deposited at the highest duty cycle of 33%, while a 31.7 nm value was reported for films generated at the lowest duty cycle, 4.8%. We did not observe trends similar to these, likely due to the differences in design between the two experimental apparatus.

IV. Discussion

The goal of the present work was to identify the optimal conditions for obtaining highly ordered films with high CF_2 content as well as to compare the structure and composition of films obtained under CW and pulsed HFPO plasma conditions. Despite the extensive study of pulsed HFPO plasmas, the CW regime has not been fully investigated. Our results show that, under the appropriate experimental conditions, fluoro-

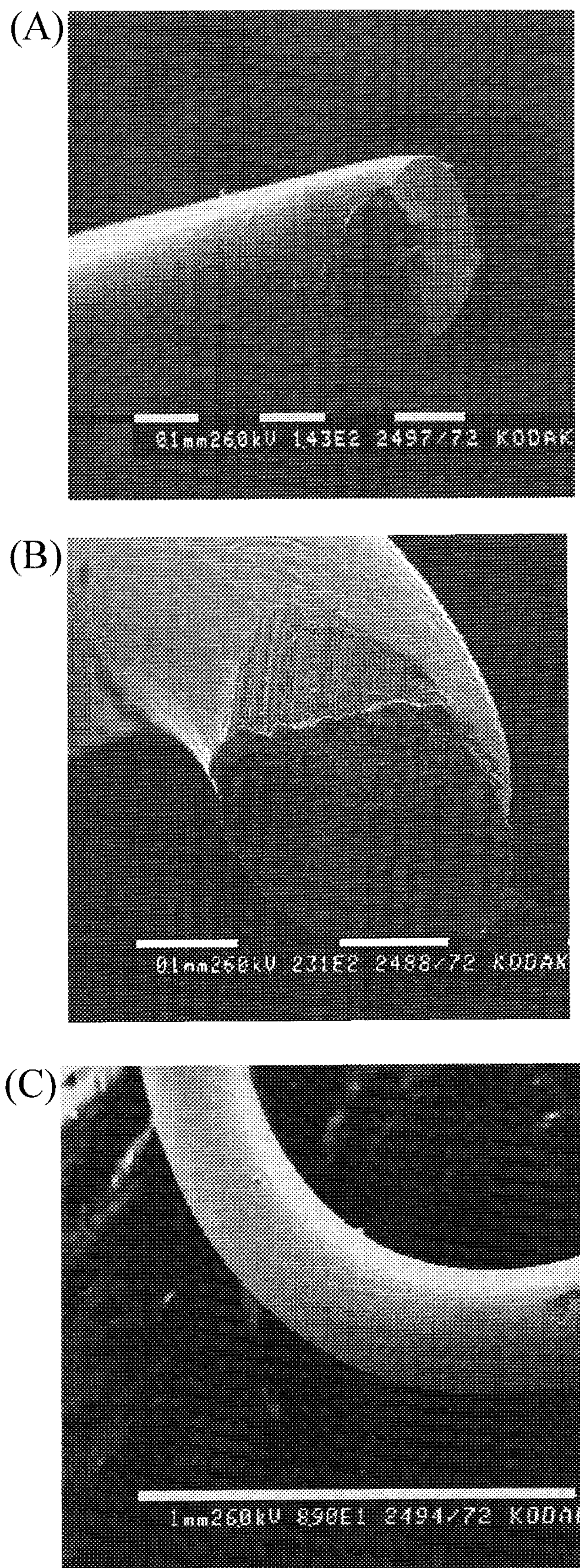

Figure 11. (a) Scanning electron micrograph of a film deposited on a 200 μm diameter Cu wire placed at position C in a 5% duty cycle pulsed plasma (magnification ×143). (b) Scanning electron micrograph of the same wire after being tied in a loop (magnification ×231). (c) Scanning electron micrograph of a film deposited on a 200 μm diameter Cu wire placed at position C in a 25 W CW plasma (magnification ×89).

(26) Labelle, C. B.; Gleason, K. K. *J. Appl. Polym. Sci.* **1999**, *74*, 2439.

carbon materials generated in CW systems display attributes virtually identical to those of films produced in pulsed plasmas. In this work, we show that films deposited far downstream from the rf glow (position C), under both CW and pulsed conditions, have the lowest degree of cross-linking and are the least amorphous. This is demonstrated convincingly by the FTIR spectra (Figures 2-4), which contain clearly separated asymmetric and symmetric stretching bands and no other features. Moreover, these compositional attributes correlate well with XPS data which show that materials generated at position C also have the highest CF_2 content and F/C ratios (Tables 1−3). Position C films also contain long CF_2 chains, as demonstrated by the SIMS data of Figure 6, which display a pronounced orientation, as determined via NEXAFS experiments. The following discussion highlights and interprets the major trends observed from our extensive parameter study and analysis.

The two experimental parameters that primarily control the type of material obtained in CW HFPO rf glows are distance from the rf coil and applied rf power. Gleason and co-workers did explore the CW power dependence in a parallel plate system but generated only amorphous films.[20] Materials generated in the glow of our CW HFPO plasmas are similar to those reported by Gleason. Unlike previous researchers, however, we have also explored the dependence of film composition as a function of distance from the HFPO plasma rf glow. While we were the first to perform distance dependence studies for materials generated in HFPO plasmas, other researchers have investigated distance effects on the composition of films generated in TFE plasma systems. Castner and co-workers found that materials deposited 10−30 cm downstream with CW rf powers < 10 W contained a high CF_2 content (~90%) and a high degree of orientation.[9] Conversely, films generated in the rf glow comprised significantly more CF_3 as well as CF groups.

Similar to Castner's results with TFE, we also discovered that the position of the substrate relative to the visible glow plays a very significant role in the type of material obtained in HFPO plasma systems. For depositions performed at position B and rf powers > 50 W, etching of the glass reactor walls occurs, as indicated by the intense SiO peak (~1100 cm^{-1}) present in the FTIR spectrum shown in Figure 2a. In contrast, materials generated at position C have IR spectra in which the dominant feature is the 1200 cm^{-1} band corresponding to CF_x stretches (Figure 2b). At lower rf powers (15, 30 W), however, no sign of reactor etching is observed for position B films, while position C materials have a low degree of cross-linking and high CF_2 content (Figure 2a and b, respectively). The composition dependence on distance from the rf glow is not surprising when one considers that many of the energetic species in the plasma, which are primarily responsible for etching and cross-linking, decay before reaching a substrate placed far downstream.[9]

The pressure dependence of the films obtained at an applied rf power of 30 W CW is also very interesting (Figure 3). At low pressures, the fluorocarbon films generated at position B are highly amorphous, as indicated by the broad IR absorbance band at 1200 cm^{-1}. At higher HFPO pressures, however, the separation between the CF_2 symmetric and asymmetric IR bands is consistent with a less amorphous fluoropolymer, similar to that deposited at position C. Increasing the pressure has a dual effect on the rf glow: both electron energy and particle mean free path decrease.[8] Both of these effects serve to decrease the amount of UV radiation reaching the deposited fluoropolymer because most excited state neutral species, which fluoresce in the UV, are created through collisions with electrons. As the electron energy decreases, the number of excited state neutrals formed decreases. Likewise, as the mean free path decreases, energy transfer occurs preferentially through molecule−molecule collisions rather than through radiative decay (emission). In addition, as the electron energy decreases, fewer ions are formed. Those ions that are created through electron impact will have less energy than the ones formed at lower pressures (higher electron energies). Thus, at higher pressures, plasma-polymerized fluorocarbon films generated at position B do not undergo as much bombardment from energetic particles as they do at lower pressures. This is also consistent with the lack of pressure dependence observed for the composition of films generated at position C, where most energetic species have already undergone recombination reactions.

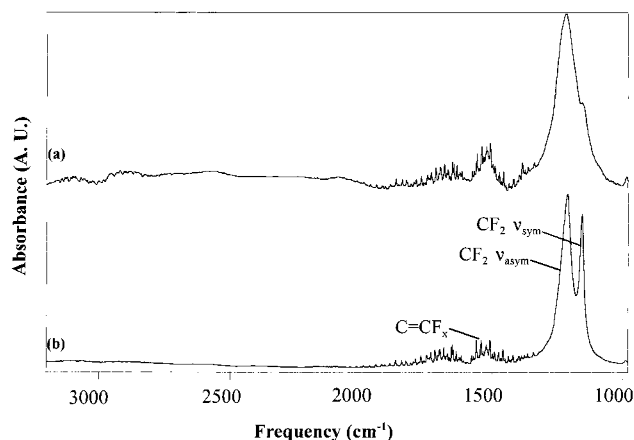

Figure 12. (a) FTIR spectrum for a film deposited 9.5 cm downstream from the rf coil with deflector plates inserted in the plasma chamber upstream from the substrate but not charged. This allows charged species to reach the substrate surface. (b) FTIR spectrum for a film deposited at the same location with one of the deflector plates charged at +200 V dc and the other grounded. This prohibits charged species from colliding with the substrate surface.

Energetic charged species are directly shown to influence the degree of film amorphousness by the FTIR spectra displayed in Figure 12. Films were generated 9.5 cm downstream from the rf coil in a 25 W CW plasma with a pair of Cu deflector plates located immediately upstream from the substrate.[27] Figure 12a shows the IR spectrum of a material deposited when the deflector plates were not charged. A broad absorption band corresponding to CF_2 vibrations is present at ~1200 cm^{-1}, suggesting the material is amorphous. Figure 12b shows the IR spectrum for a film generated when one deflector plate was biased at +200 VDC while

(27) This location is essentially the same as position B used in other experiments.

the other was grounded. The electric field thus created prevents charged species from colliding with the substrate surface. A distinct separation between the symmetric and asymmetric CF_2 IR absorbance bands is observed for materials deposited under biasing conditions, similar to what was observed for films deposited at reactor position C. The separation is not as dramatic, however, due to the presence of energetic neutral species and UV light, which are not deflected by the charged plates. The difference between the IR spectra displayed in Figure 12a and b constitutes direct evidence that charged species bombardment is primarily responsible for the formation of highly amorphous and cross-linked materials at position B.

Similar to the CW system, there are two main experimental variables that affect film composition in pulsed HFPO plasmas: duty cycle and distance from glow. Fluorocarbon polymers deposited at position C in pulsed HFPO plasmas have higher CF_2 content and a higher degree of CF_2 chain orientation than materials generated at positions A and B (Table 2). Etching of the glass reactor walls occurs at duty cycles > 5% at position A (Figure 4a and Table 3). As the duty cycle increases, however, the CF_2 content decreases and the orientation of film chains becomes less distinct in materials deposited at position C (Table 2 and Figure 8). Pulsed plasma dynamics studies show that during the on-time period radicals and charged species are created, followed by the rapid decay of short-lived ionic fragments during the off time of the pulse sequence.[28,29] The effect of energetic species on film composition and structure is significantly reduced at all reactor positions because the plasma is pulsed. With a constant on time, lower pulse duty cycles (longer off times) provide a longer time for deposition to occur unhindered by charged species effects. In addition, lower duty cycles also mean lower equivalent power applied to the plasma. Indeed, as the duty cycle increases from 5% to 33%, the CW equivalent power rises from 15 to 100 W. In a 100 W CW plasma, fluorocarbon film deposition occurs only at position C. In contrast, for the 33% duty cycle system (100 W equivalent CW power) fluorocarbon film deposition occurs at both position B and position C. One additional note is that, at higher duty cycles, we observe a more marked dependence of film composition on reactor position (Tables 2 and 3).

Angle-resolved XPS analysis results correlate well with the FTIR data and also provide additional information about composition differences between the film surface and the bulk. All the materials whose IR spectra did not contain features associated with cross-linked groups had the highest CF_2 content and F/C ratios according to XPS data. XPS analysis also showed that, for materials deposited at position C under CW conditions, the CF_2/CF_3 ratio changed from 3.5 to 6.3 when the sampling depth increased from ~20 to ~90 Å (photoelectron takeoff angle changed from 80° to 0°). Likewise, the CF_2/CF_3 ratio for films generated at position C in a 16% duty cycle pulsed plasma changed from 5.2 for surface layers to 7.2 for the film bulk at 0°. These changes suggest that the films deposited at position C in both systems have CF_3-enriched surfaces. This conclusion is further supported by static contact angle measurements which show that the surfaces of materials generated at position C are more hydrophobic than those at position B. The angle-resolved XPS and contact angle measurement information also agrees with the findings of static SIMS analysis. The former two show that position C films have CF_3-enriched surfaces, which indicates that the molecular ions of the form C_nF_{2n+1} detected in the SIMS spectrum are very likely to correspond to $(CF_2)_nCF_3$ moieties in the film. Similar conclusions were drawn by Castner and coworkers in regard to fluorocarbon materials obtained downstream from TFE plasmas. The same progression of molecular ions was observed and interpreted to indicate the presence of $(CF_2)_nCF_3$ chains.[15]

Another intriguing characteristic of the films deposited at position C is the high degree of orientation of the CF_2 chains observed for both CW and pulsed HFPO plasmas. Unlike PTFE, in which the CF_2 strands are parallel to the film surface,[15] fluorocarbon films deposited in our HFPO CW and pulsed systems at position C contain CF_2 chains perpendicular to the substrate surface. This is only the second plasma system for which this type of orientation is seen in the fluorocarbon materials generated.[15] One possible explanation for the perpendicular orientation of the CF_2 chains is the higher stability of the C−C (144 kcal/mol) bond relative to a C−Si (104 kcal/mol) bond.[30] If the film is formed through sequential addition of CF_2 moieties, this difference could lead to preferential C−C bond formation, after the first difluorocarbene groups bond to the Si surface. In contrast, the films deposited upstream do not have preferential orientation, most likely as a result of higher levels of ion and electron bombardment which lead to higher densities of chain nucleation sites.

Given the structural and compositional similarities between materials deposited in our CW and pulsed HFPO plasmas at position C, we also investigated how their flexibilities compare under mechanical stress. SEM images indicate that our films are flexible enough not to crack under the stress of bending a coated wire into a loop ~0.5 cm in diameter (Figure 11). This is the first time a high degree of flexibility was observed for films obtained in HFPO plasmas under CW conditions. Gleason and co-workers generated flexible materials in 2.4% (10/400 ms) duty cycle pulsed HFPO plasmas, but their CW films were found to crack under bending stress.[31] The difference between our CW films generated at position C and the ones studied by Gleason is that the latter were deposited at high power densities in the rf glow of a parallel plate reactor. Gleason's previous research has shown that, at high rf power, HFPO PECVD produces highly cross-linked materials which are less robust against mechanical stress than films with a low degree of cross-linking.[20] Our films deposited at position C in a 25 W CW system contain virtually no cross-linked groups, explaining their high degree of flexibility.

(28) Lin, S.; Liao, C.; Liang, R. *Polym. J.* **1995**, *27*, 201.
(29) Booth, J. P.; Hancock, G.; Perry, N. D.; Toogood, M. J. *J. Appl. Phys.* **1989**, *66*, 5251.
(30) *CRC Handbook of Chemistry and Physics*; Weast, R. C., Selby, S. M., Eds.; The Chemical Rubber Co.: Cleveland, OH, 1966; p F-130.
(31) Limb, S. J.; Gleason, K. K.; Edell, D. J.; Gleason, E. F. *J. Vac. Sci. Technol. A* **1997**, *15 (4)*, 1814.

V. Summary

PECVD using fluorocarbon systems is an extremely valuable technique in the quest for improved vapor-deposited fluoropolymers. This study shows that HFPO plasmas can be employed to produce materials with high CF_2 content and low degrees of cross-linking. In addition, our results demonstrate that pulsing the HFPO plasma is not the only route to obtaining such films. CW downstream depositions produced similar high-quality films. Note that the films generated in HFPO plasmas, similar to those seen in TFE systems, are not Teflon-like in structure. PTFE contains CF_2 moieties linked parallel to substrate surfaces, whereas the materials we deposit comprise vertically oriented CF_2 chains which are terminated in CF_3 groups. However, only films obtained at the longest distance from the plasma glow display a high degree of orientation. As observed in other plasma systems, the energetic charged species produced in the rf plasma play a crucial role in the structure and composition of the materials generated. We conclude that, with low rf powers, far downstream depositions are virtually free of undesired energetic species bombardment effects simply because these species are lost through plasma recombination processes prior to reaching a substrate. A similar result is obtained for pulsing the HFPO plasmas, despite the 300 W applied power, because charged species rapidly decay during the time off period of the pulse sequence. Further investigations of gas-phase species in the HFPO system are currently underway in our laboratories.[32]

Acknowledgment. This work was supported by the National Science Foundation. J.B. and A.M.M. also acknowledge support from the NSF-REU program. L.J.G. and D.G.C. were supported by grants from the NIH (RR-01296) and the NSF (EEC-9529161). The NEXAFS studies were performed at the NSLS, Brookhaven National Laboratory, which is supported by the DOE, Division of Materials Science and Division of Chemical Sciences. We are also grateful to Prof. Bruce Parkinson for the use of his AFM instrument.

CM0002416

(32) Butoi, C. I.; Mackie, N. M.; Williams, K. L.; Fisher, E. R. *J. Vac. Sci. Technol. A*, submitted for publication.